Remote Sensing of Environment 193 (2017) 193–203

Contents lists available at ScienceDirect

Remote Sensing of Environment

journal homepage: www.elsevier.com/locate/rse

Assessing landscape connectivity for large mammals in the Caucasus using Landsat 8 seasonal image composites

Benjamin Bleyhl [a,*], Matthias Baumann [a], Patrick Griffiths [a], Aurel Heidelberg [b], Karen Manvelyan [c], Volker C. Radeloff [d], Nugzar Zazanashvili [e,f], Tobias Kuemmerle [a,g]

[a] Geography Department, Humboldt-University Berlin, Unter den Linden 6, 10099 Berlin, Germany
[b] WWF Germany, Reinhardtstr. 18, 10117 Berlin, Germany
[c] WWF Armenia, 11/1 Proshyan Str., Yerevan 0019, Armenia
[d] SILVIS Lab, Department of Forest and Wildlife Ecology, University of Wisconsin-Madison, 1630 Linden Drive, Madison WI 53706, USA
[e] WWF Caucasus Programme Office, Aleksidze Str. 11, 0193 Tbilisi, Georgia
[f] Institute of Ecology, Ilia State University, Cholokashvili Ave 3/5, 0162 Tbilisi, Georgia
[g] Integrative Research Institute on Transformations of Human-Environment Systems (IRI THESys), Humboldt-Universität zu Berlin, Unter den Linden 6, 10099 Berlin, Germany

ARTICLE INFO

Article history:
Received 12 September 2016
Received in revised form 27 January 2017
Accepted 4 March 2017
Available online xxxx

Keywords:
Image compositing
Landsat
Image metrics
Phenology
Corridor mapping
Connectivity
Land cover

ABSTRACT

Land-use is transforming habitats across the globe, thereby threatening wildlife. Large mammals are especially affected because they require large tracts of intact habitat and functioning corridors between core habitat areas. Accurate land-cover data is critical to identify core habitat areas and corridors, and medium resolution sensors such as Landsat 8 provide opportunities to map land cover for conservation planning. Here, we used all available Landsat 8 imagery from launch through December 2014 to identify large mammal corridors and assess their quality across the Caucasus Mountains (>700,000 km^2). Specifically, we tested the usefulness of seasonal image composites (spring, summer, fall, and winter) and a range of image metrics (e.g., mean and median reflectance across all clear observations) to map nine land-cover classes with a Random Forest classifier. Using image composites from all four seasons yielded markedly higher overall accuracy than using single-season composites (8% increase) and the inclusion of image metrics further improved the classification significantly. Our final land-cover map had an overall accuracy of 85%. Using our land-cover map, we parameterized connectivity models for three generic large mammal groups and identified wildlife corridors and bottlenecks within corridors with cost-distance modeling and circuit theory. Corridors were numerous (in total, 85, 131, and 132 corridors for our three mammal groups, respectively), but often had bottlenecks or high average cost along the least-cost path, indicating limited functioning. Our findings highlight the potential of Landsat 8 composites to support connectivity analyses across large areas, and thus to contribute to conservation planning, and serve as an early warning system for biodiversity loss in areas where on-the-ground monitoring is challenging, such as in the Caucasus.

1. Introduction

Increasing human domination of the Earth has resulted in rapid losses of natural ecosystems and wildlife habitat (Butchart et al., 2010). Functioning protected areas are therefore cornerstones for conservation (Bruner et al., 2001; Macdonald et al., 2012; Watson et al., 2014), particularly for large mammals which typically have large home ranges and are attractive to poachers (Di Marco et al., 2014; Ripple et al., 2014; Ripple et al., 2015). Unfortunately, many protected areas are not large enough to support viable large mammal populations by themselves and wide-ranging species in particular depend on habitat outside protected areas (Di Minin et al., 2013; Ripple et al., 2015). This means that the landscapes between protected areas are crucial to prevent extirpation within them and that detailed information on land cover and use around protected areas is important for large mammal conservation planning (Beier et al., 2008; DeFries et al., 2007; Jones et al., 2009).

One way to overcome some of the limitations of small protected areas is to provide connectivity between them, for example through corridors (Crooks and Sanjayan, 2006; Haddad et al., 2003; Walker and Craighead, 1997). Corridors are swaths of habitat that allow movement of species among habitat patches (Beier et al., 2008; Hilty et al., 2006). Increased movement and dispersal can support both genetic exchange and range shifts, thereby mitigating effects of habitat fragmentation (Brudvig et al., 2009; Gilbert-Norton et al., 2010). Thus, corridors are an important conservation management tool to increase connectivity (Crooks and Sanjayan, 2006). Yet, delineating and assessing

* Corresponding author.
E-mail address: benjamin.bleyhl@geo.hu-berlin.de (B. Bleyhl).

http://dx.doi.org/10.1016/j.rse.2017.03.001
0034-4257/

corridors at the regional or landscape scale is challenging because it requires consistent, fine-scale, and up-to date land-cover information for large areas (Sanderson et al., 2006; Wiens et al., 2009; Zeller et al., 2012).

Remote sensing plays a key role in acquiring broad-scale environmental information for conservation planning (Pettorelli et al., 2014), and particularly Landsat imagery provide a sufficiently high spatial and temporal resolution to map land cover in a way suitable for identifying corridors. Unfortunately though, using Landsat data over large areas is often difficult due to clouds, especially in mountainous regions (Wulder and Coops, 2014). Landsat image compositing algorithms are a promising tool to overcome limitations of single-scene analyses, such as excessive cloud coverage, data gaps (e.g., through the failure of the scan-line corrector in Landsat 7 imagery), or limited data availability because of acquisition policies or archive consolidation issues. Landsat compositing algorithms mine all available imagery on a per-pixel basis to create a gap-free coverage of any user-defined study region at 30-m resolution (Griffiths et al., 2013b; Hansen et al., 2013; Potapov et al., 2011; Roy et al., 2010). Composites can be targeted to a user-defined time of the year (so-called seasonal best-pixel composites, BPC), that may be particularly well-suited to separate two or more land-cover classes (e.g., broadleaved and coniferous forest or cropland and grassland; Griffiths et al., 2013a; Roy et al., 2010). Seasonal composites are likely particularly beneficial for mapping land covers with strong phenology, because many land covers are similar in terms of their spectral properties in some times of the year, but differ in others (Baumann et al., 2012; Griffiths et al., 2013a). Existing studies so far have only tested the use of multi-seasonal data (e.g., Prishchepov et al., 2012; Senf et al., 2015) or used multi-seasonal composites (e.g., Baumann et al., 2016; Griffiths et al., 2013a), but no study tested the usefulness of seasonal composites to improve land-cover classifications empirically.

Using all available imagery allows to complement Landsat BPC with spectral metrics that summarize the full image record. For example, spectral metrics provide information on the average or variability of reflectance for a given time period (e.g., one year), or capture the minimum or maximum reflectance. Such metrics have the potential to greatly improve land-cover classifications (Griffiths et al., 2013b; Hermosilla et al., 2015; Potapov et al., 2011). Furthermore, metadata-layers can be produced containing, e.g., the number of available cloud-free observations, or zenith and azimuth of the observations used in the BPC. While Landsat composites have been applied to data from Landsat 4/5/7 (e.g., Griffiths et al., 2014; Potapov et al., 2015), increased image collection capacity may make Landsat 8 particularly suitable for large-area compositing (White et al., 2014; Wulder et al., 2015), but we are not aware of any prior studies that used Landsat 8 composites and metrics for land-cover classifications. Likewise, despite their advantages in addressing landscape-scale questions, image composites have not been derived to support large mammal conservation planning.

One region that harbors a range of iconic and wide-ranging large mammal species is the Caucasus at the intersection of Europe, the Middle East, and Central Asia. However, land-use pressure in the Caucasus is widespread and increasing, especially in the form of agriculture, infrastructural development, mining, logging, and tourism (Williams et al., 2006). All this raises concern about land-use effects on wildlife populations and habitats, suggesting that conservation opportunities may be diminishing as land use intensifies (Zazanashvili et al., 2012). Many of the iconic large mammals such as the European bison, the Persian leopard, and the Eurasian lynx occurred in the past in large parts of the region, but their current distributions are only a fraction of where they occurred before, and they require conservation action (Bleyhl et al., 2015; Khorozyan and Abrarnov, 2007; Zazanashvili et al., 2012). Moreover, conservation planning is challenging because the Caucasus extends into six countries (i.e., Russia, Georgia, Armenia, Azerbaijan, Turkey, and Iran), creating the necessity of ecoregion-wide coordination. Despite numerous local conservation initiatives and a trans-national conservation plan (Montalvo Mancheno et al., 2016; Williams et al., 2006; Zazanashvili et al., 2012), implementing conservation planning at broad scales is currently severely hindered by a lack of up-to-date, fine-scale land-cover information that is consistent across political borders and that may be used to identify bottlenecks for connectivity (CORINE land cover, for example, only covers European Union countries). The Caucasus is therefore an interesting region to test new approaches for broad-scale land-cover mapping and how they could enable connectivity assessments.

Our goal here was to utilize the full Landsat 8 image data record from launch (April 2013) to December 2014 to assess landscape connectivity for large mammals across the entire Caucasus ecoregion. Specifically, our objectives were to (1) test the usefulness of seasonal Landsat 8 image composites and spectral metrics for land-cover classifications, (2) map land cover across the Caucasus, (3) identify potential wildlife corridors between protected areas in the Caucasus ecoregion, and (4) highlight potential bottlenecks that jeopardize landscape connectivity.

2. Methods

2.1. Study area

The Caucasus ecoregion is located between the Black and Caspian Seas. We analyzed the Caucasus ecoregion as defined by the World Wide Fund for Nature (WWF; Krever et al., 2001) plus a buffer of 30 km to avoid edge effects (760,000 km^2; Koen et al., 2010). The ecoregion's topography includes mountain ranges (e.g., the Greater and Lesser Caucasus, the Talysh Mountains), plains, mainly north of the Greater Caucasus and in the eastern part, and upland areas in the central part. Climate varies from moist and temperate in the west (>2000 mm precipitation) to arid in the east (<250 mm). Forests occur mainly in the mountains and are dominated by broadleaved tree species (mostly beech (*Fagus orientalis*), oak (*Quercus* spp.), hornbeam (*Carpinus betulus, Carpinus orientalis*), and chestnut (*Castanea sativa*)). Additionally, the region harbors large steppe areas, as well as semi-deserts and arid woodlands in the drier eastern parts (Krever et al., 2001).

Agricultural land use has a long history in the Caucasus and is economically important. During Soviet times, agriculture in Armenia, Azerbaijan, Georgia, and Russia was characterized by large state farms. Today, most farms in Armenia and Azerbaijan are private with small fields, whereas in Russia and Georgia parts remained as larger state or corporate farms (Giovarelli and Bledsoe, 2001; Lerman et al., 2004). Main crops include cereals, vegetables, fruits, tea, and tobacco. In the mountainous regions, livestock production is also important (Williams et al., 2006).

The Caucasus is a key region for the conservation of large mammals. In the late 1980s and '90s, large mammal populations declined dramatically, mostly due to poaching and weak law enforcement during the political and economic transition period from communism to market economies (Bragina et al., 2015; Williams et al., 2006; Zazanashvili et al., 2004). Since the early 2000s, wildlife populations have recovered somewhat, but land-use change, mining, and infrastructural development, as well as ongoing political and armed conflicts threaten this recovery. New protected areas have been established in the last two decades, yet it remains unknown how well protected areas are connected across the region.

2.2. Image compositing

To map the land cover of the Caucasus ecoregion, we applied pixel-based image compositing (Griffiths et al., 2013b). We acquired all available Landsat 8 images from April 12th 2013 to December 18th 2014 for the 63 Landsat footprints covering our study area. We downloaded terrain-corrected images with <70% cloud cover as the Landsat Surface Reflectance High Level Data Product (i.e., Landsat 8 bands 1–7), as well as the surface temperature product provided by

the USGS (i.e., Landsat 8 bands 10 and 11; in total > 2000 images; downloaded in April 2015 from: https://espa.cr.usgs.gov). To create best pixel composites, we used a score-based weighing function to assess each pixel's suitability for the final composite, based on acquisition year, day of year, distance to clouds, thermal brightness temperature, and distance to nadir for the Landsat 8 bands 2–7, resulting in 6-band composites consisting of pixels with the highest suitability score (Griffiths et al., 2013b). The thermal brightness temperature was incorporated into the scoring, assuming that warmer pixels are less likely to be affected by cloud remnants or haze. Distance to clouds was based on the cloud mask delivered with the Surface Reflectance Product (i.e., the C Language Function of Mask cloud mask or CFmask) and calculated as the number of pixels to the nearest cloud or cloud shadow. As our target year we chose 2014, meaning that pixels from that year were favored over pixels from 2013. To capture different phenological stages of the vegetation, we produced seasonal composites that were based on all available observations, but employed different target days of year for the compositing (i.e., pixels close to that day were favored). The output from the pixel-based compositing algorithm were four cloud-free image composites, one for spring, summer, fall, and winter (defined by the target days of year: 105 for spring, 196 for summer, 288 for fall, 349 for winter). Each of these composites consisted of 6 spectral bands (i.e., bands 2–7).

In addition to the best-observation composites, we calculated spectral metrics and metadata flags for each pixel. The spectral metrics were based on all clear observations and thereby contain information on phenology of the land-cover classes over time (e.g., band-wise mean and standard deviation surface reflectance; Griffiths et al., 2013b). In total, our compositing resulted in 93 bands (see Table S1 for a full list).

2.3. Assessing the value of seasonal composites and spectral metrics for land-cover mapping

We classified nine land-cover classes: coniferous forest, broadleaved forest, mixed forest, rangeland (including pastures), cropland, built-up, sparse vegetation, permanent ice and snow, and water. We collected training data using current high-resolution GoogleEarth images in combination with the full set of Landsat 8 composites, digitized training data polygons, and randomly sampled 4000 training points within these polygons for each class. Training data for built-up, permanent ice and snow, and water was gathered based on visual interpretation of the high-resolution imagery. For the forest classes, if available in GoogleEarth, we also considered imagery from leaf-off seasons. We identified cropland areas visually based on their rectangular shape, plowing patterns, homogeneous texture, and signs of bare soil in spring. Conversely, we labeled areas as rangeland that did not show rectangular shape, evidence of plowing, or bare soil in spring. The sparse vegetation class was defined as not showing a clear vegetation signal (i.e., spectral profile) in any of our Landsat composites or being clearly identified as bare areas due to the presence of rocks, cliffs, or sandy areas in the GoogleEarth high-resolution images. After initial classifications, we added additional training data iteratively in misclassified areas.

To test the usefulness of the seasonal composites, we ran initial classifications based on single-season composites and all possible combinations of seasonal composites. For the classification, we used a Random Forests classifier with 300 trees. Random Forests are a machine-learning algorithm (Breiman, 2001) that consistently outperform parametric classifiers (Gislason et al., 2006) while being computationally efficient. To validate the land-cover maps of our alternative classification runs, we randomly collected 200 points per class (strata derived from the classification using all bands), and labeled them individually according to visual inspection of current (2010 or later) high-resolution GoogleEarth imagery in conjunction with our Landsat composites. We assessed composite-combinations using standard accuracy measures (Foody, 2002).

To assess the extent to which the spectral metrics and metadata flags improved classification accuracy, we took the best-performing seasonal composite combination and compared it to classifications that included also the spectral metrics, the metadata flags, and both. We used the best-performing classification run to generate our final land-cover classification and applied a McNemar's test to assess if differences in accuracy between the classifications were significant (De Leeuw et al., 2006).

For our final land-cover map, we applied a minimum mapping unit of 0.54 ha (six Landsat pixels) to remove salt-and-pepper structures that mainly represented misclassifications. Furthermore, we used point locations of settlements (i.e., one point location per settlement) from Open Street Map (OSM; http://www.openstreetmap.org/) to improve the discrimination between the built-up and sparse vegetation classes. We limited built-up to areas within 1 km around the OSM settlement point layer and assigned built-up pixels outside this buffer to the sparse vegetation class. To validate our final land-cover map, we calculated overall accuracy and class-wise user's and producer's accuracy (Foody, 2002). We accounted for potential sampling bias by adjusting error and area estimates according to the class distribution of our target classes (Olofsson et al., 2014).

2.4. Corridor mapping

To assess landscape connectivity and to map corridors, we converted our land-cover map into a resistance surface that measured how difficult it is for a given species to move through the landscape (Zeller et al., 2012; Ziółkowska et al., 2014). We selected all eleven large mammal species as focal species identified as priority species in the Caucasus Ecoregion Conservation Plan (Table 1; Zazanashvili et al., 2012). A key step for assessing connectivity using resistance surfaces is setting resistance values for each land-cover class. This is best done using movement data for the species in question (Ziółkowska et al., 2016a) but such data are rarely available and expert-knowledge can be an alternative (Beier et al., 2008). To obtain expert knowledge, we conducted an email survey among 27 wildlife experts in the Caucasus, asking them to assign resistance values for each combination of focal species and land-cover class.

Table 1
Species in the three dispersal groups.

Dispersal group	Species		Number of expert scorings
#1: Forest-and-shrubland group	Brown bear	*Ursus arctos*	16
	European bison	*Bison bonasus*	8
	Persian leopard	*Panthera pardus saxicolor*	15
	Eurasian Lynx	*Lynx lynx*	14
	Caucasian red deer	*Cervus elaphus maral*	13
#2: Open-land group	Goitered gazelle	*Gazella subgutturosa*	12
	Striped hyena	*Hyena hyena*	14
	Gmelin's mouflon	*Ovis ammon gmelini*	13
#3: Mountain group	Bezoar goat	*Capra aegagrus*	14
	Caucasian chamois	*Rupicapra rupicapra caucasica*	10
	Caucasian tur	*Capra cylindricornis* & *Capra caucasica*[a]	11

[a] Considered as one species for the purpose of our analysis.

Table 2
Resistance values for the land-cover classes used to parameterize the cost surface for the connectivity analysis. Values refer to the minimum, median, and maximum resistance values per focal species cluster according to our wildlife expert survey.

		Resistance values[a]					
		Coniferous forest	Broadleaved forest	Mixed forest	Rangeland	Cropland	Sparse Vegetation
Forest-and-shrubland	min	1	1	1	2	5	5
	median	1	1	1	3	7	7
	max	3	2	2	4	9	8
Open-land	min	7	7	7	1	4	2
	median	7	7	8	1	5	3
	max	9	10	10	2	5	3
Mountain	min	4	4	3	2	7	2
	median	4	5	4	4	8	3
	max	6	6	6	5	8	7

[a] The land-cover classes built-up, permanent ice and snow, and water formed total barriers (i.e., no movement through these covers was allowed in our analysis).

Resistance values were allowed to range from 1 (most permeable) to 10 (least permeable). In total, we received 17 responses (return rate of 63%; Table 1).

Our goal was to identify corridors that would benefit many species, which is why we assigned the eleven species to broad dispersal groups. To do so, we first calculated the median resistance values for each land-cover class and species based on all expert scorings. We used the median to account for variability in expert scorings (Fig. S1). Second, we used a k-means clustering analysis to derive three clusters of focal species that were similar in terms of their dispersal limitations. We discussed and further verified these dispersal groups in a workshop with Caucasian wildlife experts held in Berlin in February 2016. We labeled the dispersal groups according to movement traits of the species within each group as 'forest-and-shrubland species', 'open-land species', and 'mountain species'. For each of these three groups, we delineated three resistance surfaces representing the minimum, median, and maximum resistances of the species in a specific group (Table 2).

We further added barriers that are known to inhibit dispersal to our resistance maps. As partial barriers, we used motorway, trunk, and primary roads, as mapped in OSM, as well as elevations above 3000 m (approximately the sub-nival zone in the Caucasus). We assigned resistance values of 100 to these barriers. We tested for sensitivity of this cost parameter by also testing cost values of 50, 200, and 500, revealing only slight changes in corridor distributions (Fig. S2). As total barriers (i.e., no-data in the connectivity analyses), we considered the land-cover classes built-up, permanent ice and snow, and water, as well as areas above 4000 m (the limit of vascular plant growth; Zazanashvili et al., 2000). Although some of our species can occur above 3000 m, and at least temporarily above 4000 m, many areas in the Caucasus at this elevation do not foster vascular plant growth or are permanently glaciated, severely hindering the movement of most species. We therefore chose to use elevation barriers to avoid overestimating connectivity or deriving unrealistic corridors.

We mapped corridors between Caucasian protected areas of IUCN category I and II based on the World Database on Protected Areas (IUCN and UNEP-WCMC, 2015) and WWF's Caucasus Programme Office database (wwfcaucasus.net; Fig. S3). We focused on only these IUCN categories because protected areas with lower protection status rarely contained any of the species we focused on in our study. Protected areas (PAs) bordering each other were considered as one PA. Disjunct patches of the same PAs were modeled as one patch if patches were <10 km apart and as separate patches otherwise (resulting in 57 PAs in total). In order to exclude PAs without forest cover for the forest-and-shrubland group, we only considered PAs with forest cover >10% for that group (resulting in 41 PAs in total; we chose 10% as our threshold because some species from that group such as Eurasian lynx or brown bear occur in areas with 11% forest cover). We calculated cumulative resistances for the closest protected area pairs using the Linkage Mapper Toolkit (McRae and Kavanagh, 2011), resulting in least-cost paths (i.e., the single pixel-wide path between each PA pair with the lowest cumulative resistance) and corridors around them (i.e., those areas around least-cost paths with a cumulative resistance below a certain threshold; Ziółkowska et al., 2016b). For each path, we calculated the ratios of (a) the cost-weighted distance divided by the Euclidean

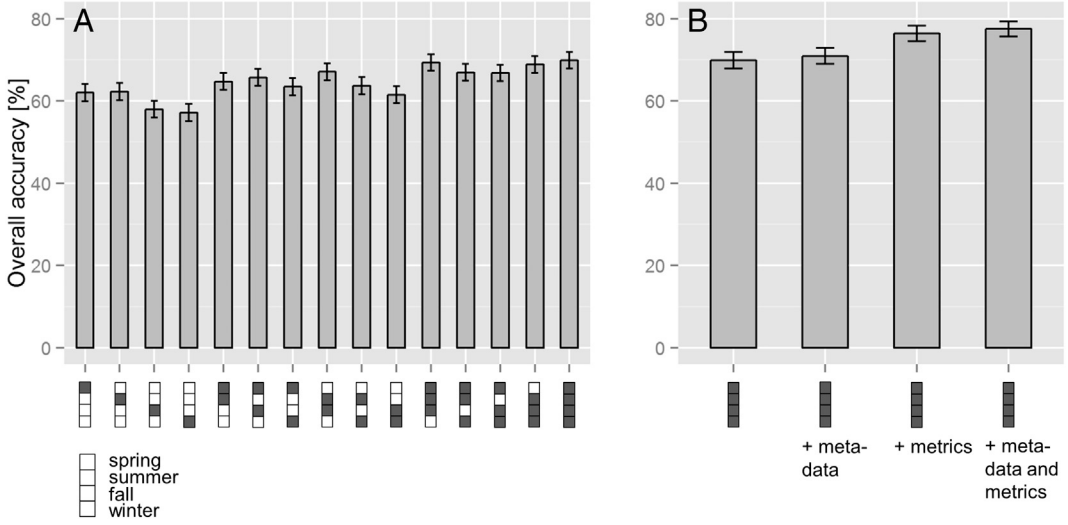

Fig. 1. Overall acurracies of different composite combinations: (A) across all combinations and (B) comparing the four seasons plus metadata and metrics. Filled boxes indicate the seasonal composites that were used. Error bars show the 95% confidence intervall.

distance and (b) the cost-weighted distance divided by the least-cost path distance as indicators of corridor quality (Dutta et al., 2015). High values of these indices indicate low corridor quality. To identify bottlenecks within our corridors, we applied circuit theory using the Pinchpoint Mapper tool within the Linkage Mapper Toolkit (McRae et al., 2008). This tool uses Circuitscape to model connectivity based on concepts from electric circuits where landscapes consist of nodes, resistors between them, and a current density flowing from node to node (McRae et al., 2013). This current density can be interpreted as the likelihood of a species passing through a cell, with high current indicating a lack of alternative routes and therefore a bottleneck in a corridor (McRae, 2012). Although such bottlenecks can be identified well in current density maps, there is at the moment no systematic way to validate bottlenecks (Pelletier et al., 2014). We defined bottlenecks here as areas with current density of the mean plus two standard deviations. Because the connectivity modeling is computationally very demanding, and initial results for smaller sub-regions at coarser resolutions were qualitatively similar to fine resolutions, we ran all connectivity models at a 300-m resolution.

3. Results

3.1. Comparison among seasonal composites and spectral metrics

We generated four seasonal best-pixel composites (spring, summer, fall, and winter 2014) at 30-m resolution over a heterogeneous area of 760,000 km^2. Although using >2000 images with at least 10 images per footprint, there were a few areas without any clear-sky observation (0.17% of all pixels). These areas were excluded from further analyses.

Our comparison of different composite combinations revealed highest overall accuracy (OA; 69.9%) when using all four seasonal composites together (Fig. 1). The spring and the summer composite resulted in the highest accuracies when using only one season for the classification (62.0% and 62.3%, respectively). When we used two seasons, combinations that included the summer and fall composite performed best (Fig. 1), and the McNemar's tests showed that these differences to other two-season combinations were significant ($p < 0.05$) except to the spring-fall combination. When using three seasons, the spring-summer-fall combination outperformed other combinations ($p < 0.05$). Despite having the highest overall accuracy, using all four seasons together was not significantly better than using a three-season combination that included the summer and fall composites ($p > 0.05$; see Tables S2–S4 for full McNemar's test results).

To assess the value of spectral metrics and metadata layers for our land-cover classification, we added them to the four season composites. Adding the spectral metrics improved accuracy significantly (Fig. 1; OA from 69.9% to 76.4%; $p < 0.001$). Accuracy of the land-cover maps based on all seasons plus the metadata was slightly, but not significantly, higher than for the four seasons by themselves. Similarly, adding the metadata layers to the four seasons plus spectral metrics led to a higher accuracy but not to a significant change. Because the land-cover map based on the four seasons plus spectral metrics and metadata layers yielded the highest overall accuracy (77.5%), we chose this combination as our final land-cover map.

3.2. Land-cover mapping

After applying our post-classification steps (minimum mapping unit and built-up area correction), the overall accuracy of this map was 84.8% (Table 3). Single-class user's accuracy ranged from 71.8% to 100% (for the sparse vegetation and the water class, respectively) and producer's accuracy from 20.5% to 97.4% (for the built-up and the water class, respectively). Our land-cover map highlighted extensive cropland areas, mainly in Russia, north of the Greater Caucasus (Fig. 2). Rangeland was the most widespread class (300,000 km^2 or 39% of the study area; numbers are rounded, see Table 3 for exact numbers) followed by cropland (190,000 km^2; 25%), water (100,000 km^2; 13%), and broadleaved forest (90,000 km^2; 12%; Table 3). All three forest classes together covered an area of 120,000 km^2. Forest was mainly found in mountainous regions (72% of forest >500 m) and primarily consisted of broadleaved trees (74% of all forest). Coniferous forest was mainly found above 1500 m. About 8% of the forest in the ecoregion was protected. In general, protected areas were mainly composed of forest and rangeland (each class covered 39% of the total protected land). Croplands were concentrated at lower elevations (72% <500 m).

3.3. Wildlife corridors

Using the three large mammal dispersal groups that emerged from our expert survey and subsequent clustering, we generated three resistance surfaces for each dispersal group, corresponding to the minimum, median, and maximum resistance values per group. These maps did not result in substantially different corridors and we here therefore only show results for the median value (see Fig. S4 for the other values). In total, we identified 348 potential wildlife corridors linking protected areas (Fig. 3). Euclidean distances among protected areas ranged from 0.6 to 333 km (mean: 60 km, standard deviation: 52 km). Corridor length also varied substantially (e.g., least-cost path length ranging from 0.9 to 410 km; Table 4). Corridors for the forest-and-shrubland and for the open-land dispersal groups were on average shorter than for the mountain group (73 km and 67 km mean least cost path length, respectively, versus 78 km for the mountain group) and of better quality. Quality was on average highest for the forest-and-shrubland group (Table 4). While low-quality corridors for the forest-and-shrubland group were mainly located in the eastern part of the study region, there was no such pattern for the other groups (Fig. 4).

Bottlenecks were common within our corridors (Fig. 3). Some narrow corridors were almost entirely classified as bottlenecks indicating that these corridors may have limited ecological functionality. For example, the corridors between Prielbrusie National Park and Severo-Osetinsky Zapovednik and Alania National Park entailed bottlenecks for all dispersal groups (inserts A, C, and E in Fig. 3). Additionally, many corridors had very

Table 3
Overall and class-wise accuracies, adjusted for potential sampling bias.

Overall accuracy [%]	Land-cover classes	Class-wise accuracies [%]		Adjusted area estimation [km^2]
		Producer's accuracy	User's accuracy	
84.8	Coniferous forest	60.2	83.8	15,574
	Broadleaved forest	84.6	79.8	89,504
	Mixed forest	56.9	76.2	16,023
	Rangeland	84.1	87.6	300,751
	Cropland	90.4	78.2	192,782
	Built-up	20.5	91.3	13,254
	Sparse vegetation	66.3	71.8	26,036
	Ice & permanent snow	92.0	89.0	2104
	Water	97.4	100.0	101,133

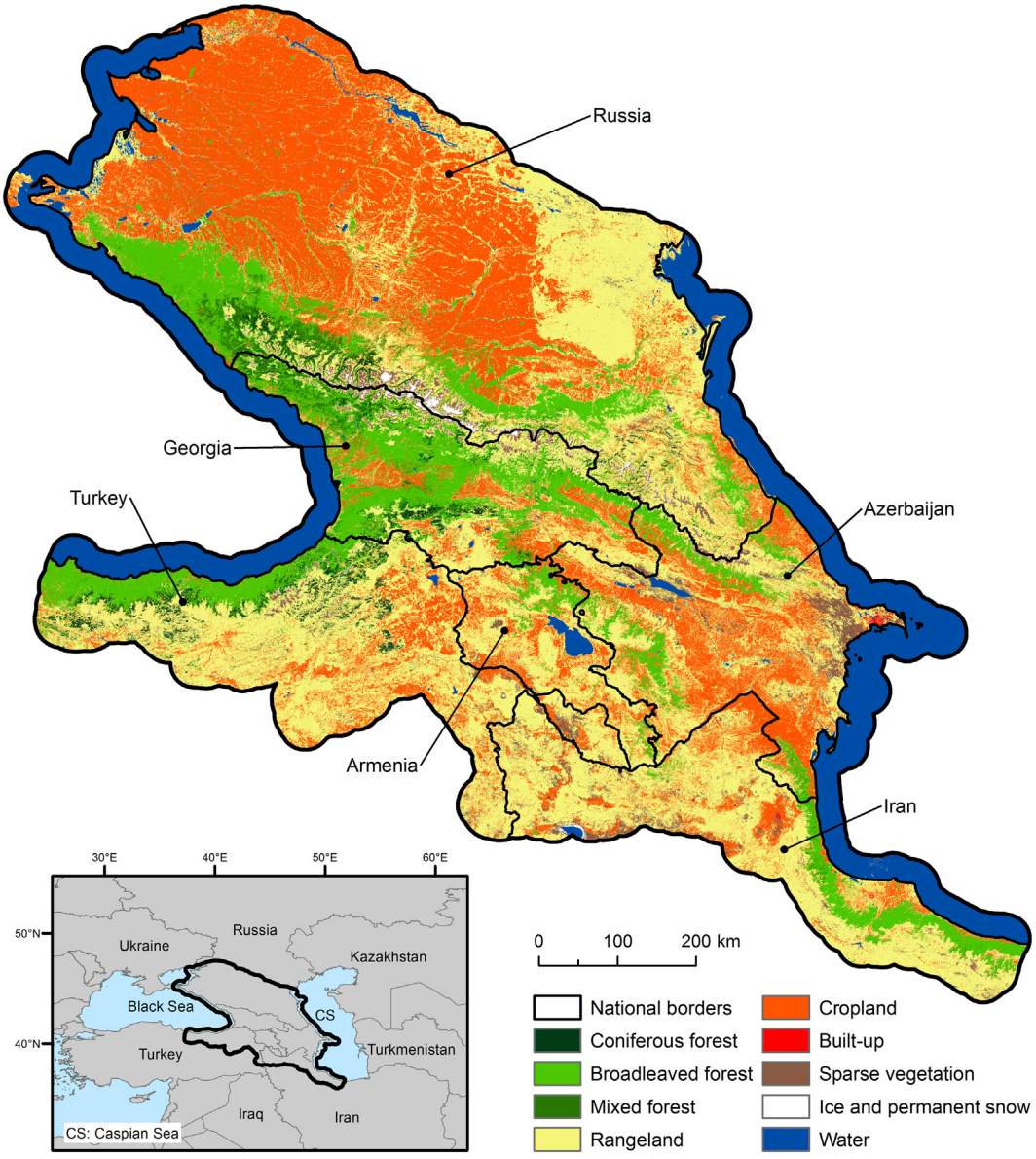

Fig. 2. Land cover of the Caucasus region. Inset shows the location of the study area between the Black Sea and the Caspian Sea.

narrow swaths of relatively low travel costs (e.g., some of the north-south leading corridors for the open-land and mountain groups).

4. Discussion

Land-use and land-cover change is a main cause of biodiversity loss globally, and conservation planning depends on up-to-date and fine-scale land-cover maps from remote sensing. This is particularly the case for large mammals, which require large core habitats, and functioning corridors between them to persist in increasingly human-dominated landscapes. The launch of Landsat 8, with its improved radiometric resolution and imaging capacity, along with new algorithms that allow making best use of all available imagery, provide opportunities to support conservation planning with remote sensing. We demonstrate this by deriving, to our knowledge, the first seasonal large-area image composite from Landsat 8 imagery, which we used to map land cover and wildlife corridors across the Caucasus ecoregion, a global biodiversity hotspot.

Our results highlight the value of temporal information for mapping land cover across complex landscapes. Multiple seasonal composites resulted in better classifications than using only a single-season composite, and adding spectral metrics that capture information from all available clear observations further improved the accuracy of our land-cover classifications.

Based on our land-cover classes and expert scorings we derived three large mammal dispersal groups for which we mapped corridors among protected areas. Corridors were widespread but often had bottlenecks indicating limited functioning and a high threat to loosing connectivity without adequate protection and restoration measures. Because large mammals require extensive habitats, conservation planning requires identifying and safeguarding corridors between core habitat areas that are typically located inside protected areas. Our analysis thus demonstrates how Landsat 8 compositing can contribute to such broad-scale conservation planning by providing key environmental information to map corridors at fine scale across large areas.

4.1. Mapping land cover using seasonal Landsat 8 composites

We achieved the highest overall accuracy using image composites from all four seasons (i.e., spring, summer, fall, and winter). This

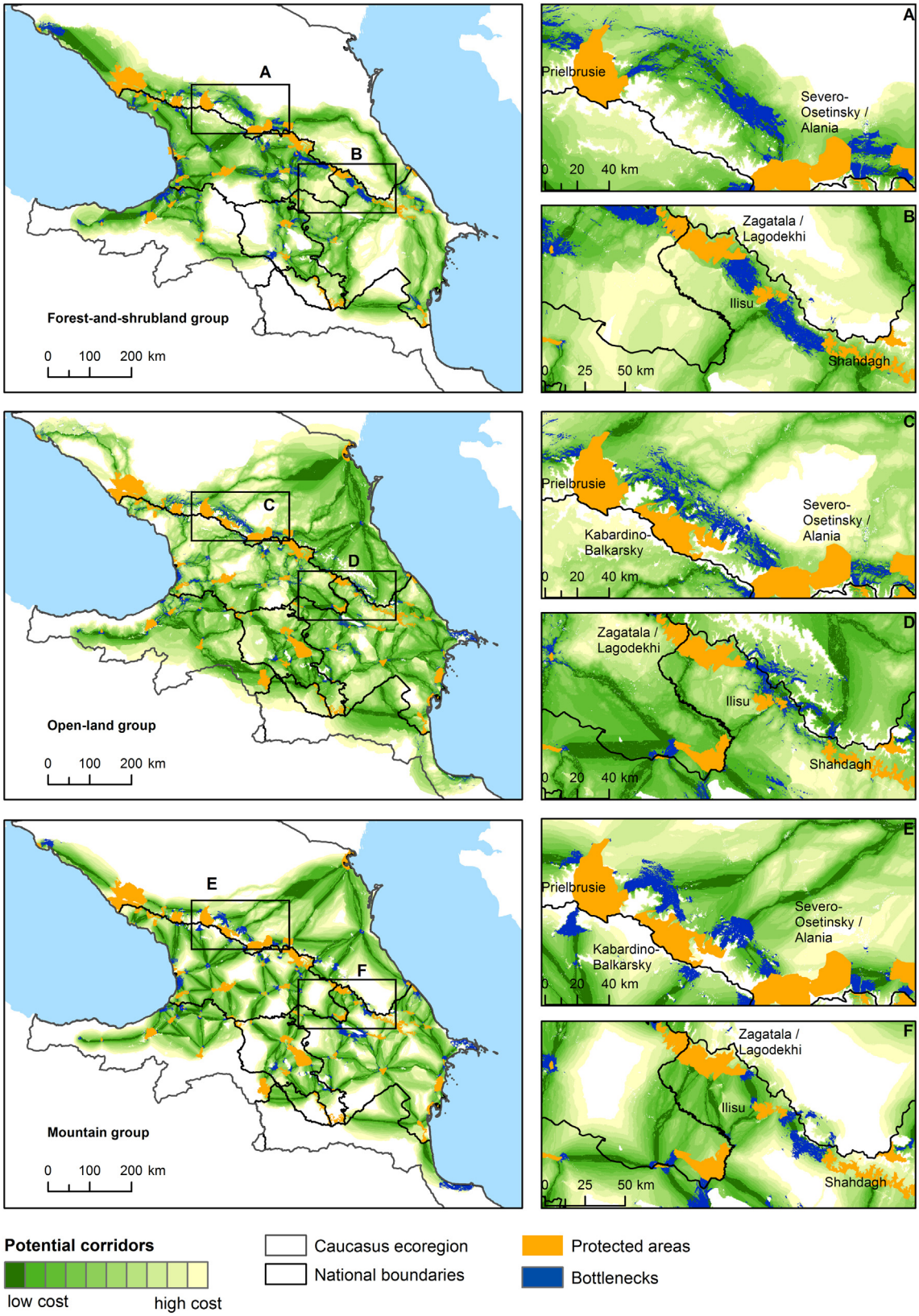

Fig. 3. Least cost corridors and bottlenecks among protected areas with IUCN category I and II. Corridors were normalized to the respective least-cost path and therefore low cost refers to areas of low travel cost. For visualization purposes, corridors were clipped to a cutoff width of 100 km (i.e., the maximum corridor width is set at cells with a 100-times higher cumulative cost-distance than that of the respective least-cost path (McRae and Kavanagh, 2011)). Bottlenecks in the map were identified as areas with current density higher than the mean plus 2 standard deviations (see Fig. S5 for maps showing the continuous current density).

Table 4
Corridor properties for the three generic dispersal groups.

	Least-cost path length [km]		Cost-weighted distance [km]		Ratio of cost-weighted divided by Euclidean distance		Ratio of cost-weighted distance divided by least-cost path length	
	Range	Mean (±sd)	Range	Mean (±sd)	Range	Mean (±sd)	Range	Mean (±sd)
Forest-and-shrubland group	0.9–409	73 ± 74	0.9–946	143 ± 192	1.07–6.85	2.32 ± 1.25	1.00–4.13	1.72 ± 0.75
Open-land group	2–384	78 ± 63	5–883	127 ± 118	1.02–21.41	2.62 ± 2.23	1.00–7.00	1.75 ± 1.00
Mountain group	0.9–368	67 ± 58	5–1595	298 ± 261	3.45–40.92	5.57 ± 3.43	3.19–9.20	4.54 ± 0.83
All groups combined	0.9–409	72 ± 64	0.9–1595	195 ± 215	1.02–40.92	3.67 ± 2.98	1.00–9.20	2.80 ± 1.62

underlines the importance of multi-temporal imagery and therefore considering different phenological vegetation stages when classifying land cover (Griffiths et al., 2014; Müller et al., 2015; Senf et al., 2015). Composite combinations that included summer and fall composites always yielded higher overall accuracies than other combinations, suggesting that important phenological characteristics are captured in these seasons. For example, cropland might show bare soil in fall after being harvested while high reflectance in summer likely further helps to distinguish it from rangeland and other classes. Additionally, using images from different seasons is well suited to separate between forest and cropland (Baumann et al., 2012). Combinations with the winter composite did only marginally improve classification accuracy, likely due to higher similarity among some classes (e.g., less green vegetation on rangeland and cropland).

Studies mapping land uses such as farmland abandonment have previously pointed out the usefulness of jointly using Landsat images from summer, fall, and spring (e.g., Baumann et al., 2011; Prishchepov et al., 2012), and our test of phenological composites supported this finding.

Similarly, adding spectral metrics to the seasonal composites further improved classification accuracy significantly. Spectral metrics capture information on the variability and distribution of imagery *within* a phenological cycle, complementing the information entailed in the seasonal composites (Griffiths et al., 2013b; Potapov et al., 2011). Higher variability might for example help to distinguish rangeland areas from built-up areas that contain green spaces. Additionally, image metrics are useful to compensate for compositing artifacts and to reduce salt-and-pepper patterns in classifications since they are based on all clear observations (Griffiths et al., 2013b). Conversely, adding the metadata flags led only to a minor, and in our case insignificant, increase in accuracy which may indicate that spectral features alone contained sufficient information to separate the classes of interest well. For our classification problem, the metadata information, such as the number of clear observations or the day of year of image acquisition, did thus not add additional information that helps to discriminate land cover, which could be different though in more data-sparse situations. In sum, given that compositing algorithms and the calculation of spectral metrics are highly automated, we recommend to analyze at least three

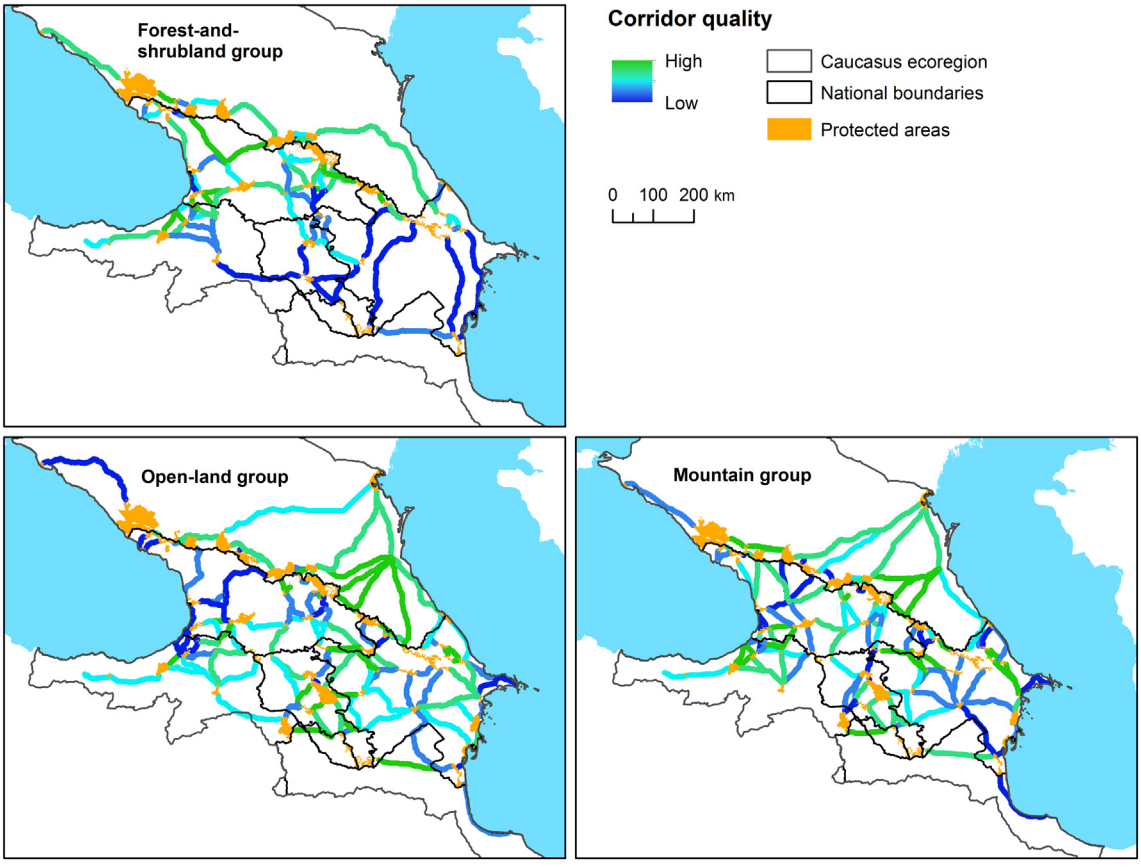

Fig. 4. Corridor quality calculated as the ratio of cost-weighted and Euclidean distance. Low quality indicates a high cost-weighted compared to the Euclidean distance between two protected areas. Our second quality index showed similar patterns (Fig. S6).

seasonal composites, and to include spectral metrics that capture distributional features of the imagery, when mapping land-cover for large areas based on Landsat-like sensors.

Our classification resulted in a reliable land-cover map despite the high heterogeneity of our study area. Nevertheless, a few sources of uncertainty need mentioning. First, despite having at least ten images per footprint available, there were areas without any clear-sky observation. Because these areas were clustered in the very high mountain areas (i.e., areas which we mostly masked out later because they do not allow for movement of large mammals due to harsh conditions), we do not expect strong effects on our analyses. Nevertheless, more data might have helped to better distinguish between sparse vegetation and built-up areas based on phenology differences between the classes. Second, the spectral similarity of the built-up and sparse vegetation classes led to a high commission error of the built-up class in initial classification runs. Settlements often entail areas of open soil and building materials can spectrally be similar to bare areas such as rocks, leading to confusion between built-up and sparse vegetation classes. In our case, using a masking approach for built-up areas (i.e., limiting classified built-up areas to within 1 km distance to the Open Street map settlement point layer), solved this problem and improved accuracy. In situations where ancillary data are unavailable, generating composites for multiple years or longer time periods (1.5 years in our case) may result in a higher spectral separability of built-up and sparse vegetation classes. Third, for our seasonal composites, we chose the target days of year to approximate different phenological stages of the vegetation. Because the timing of seasons (i.e., the day of year) varies across years, identifying key phenological dates such as the minimum and maximum peaks of vegetation greenness beforehand instead of using day of year approximations may further improve land-cover classifications (Estel et al., 2015; Senf et al., 2015).

4.2. Mapping wildlife corridors

Based on our land-cover map, we delineated resistance surfaces for three large mammal species groups (labeled as forest-and-shrubland, open-land, and mountain group) to identify corridors among protected areas in the Caucasus. Clustering species with similar dispersal ability reduced the number of individual assessments necessary to derive corridors. This means that our corridors are largely generic, and thus potentially valuable for more species than those that were explicitly included in our dispersal groups.

Corridor properties differed among the three dispersal groups. Corridor length was on average shorter for the forest-and-shrubland and the open-land groups and quality was highest for the forest-and-shrubland group. The short length and better quality of corridors for the forest-and-shrubland group suggests that protected areas are relatively well connected through forest. This is also highlighted by the low corridor quality for the forest-and-shrubland group in eastern and southern parts of the study area, where forest cover is naturally lower. Nevertheless, many corridors are substantially longer than the distances that single movement events of our species typically would cover. Our corridors should be interpreted as starting points for managing towards a better connected network of protected areas and more detailed analyses would be needed to assess if corridors do facilitate movement of individuals, and where conservation action such as habitat restoration is needed (Beier et al., 2008).

While we found numerous corridors, bottlenecks were common in most of them. Many of the corridors that connected protected areas in close proximity to each other had such bottlenecks. Bottlenecks can be a result of limited availability of permeable land-cover, of passages severed by roads, or a combination of both factors. Nevertheless, current density (i.e., the unit to identify bottlenecks with Circuitscape) is commonly higher between protected areas in close proximity (Dickson et al., 2013) which might lead to wider bottlenecks so that additional measures are needed to assess corridor quality, particularly for short corridors (e.g., corridor width or our quality indices). Bottleneck areas are candidates for immediate conservation actions, because the loss of them can lead to a collapse of connectivity in habitat networks (Dutta et al., 2015). Only about half of the corridors that we mapped were of high quality, further stressing that connectivity between many protected areas might already be limited.

Integrating information across focal species to derive general wildlife corridors is a challenging task. Our expert-based clustering approach showed how general corridors can be derived when available data are scarce. However, our method has a few drawbacks. First, least-cost analyses always identify the best corridor between protected areas regardless of their potential functionality (Beier et al., 2008). Thus, our corridors will have to be validated on the ground, for example with trail cameras. Third, land cover was our main variable in determining the resistance surface. This greatly simplifies the complex decisions related to animal movement, which are also affected, for example, by fine-scale resource availability, predation, or human disturbance. Fourth, expert scorings of resistance values varied markedly for some land-cover classes and for some species. We used median values for each scoring to reduce subjectivity, but we cannot fully rule out bias on our corridors due to the expert scoring. Finally, while analyses based on expert scorings are common (Beier et al., 2009; Zeller et al., 2012), it would be better to have actual movement data. However, such data do not exist for the Caucasus. We tried to minimize subjectivity by surveying many experts, and by grouping species (Beier et al., 2008), but we cannot fully rule out remaining biases.

5. Conclusions

Seasonal Landsat 8 image composites allowed us to reliably map land cover across a large and highly heterogeneous area, an important prerequisite for broad-scale connectivity analyses. Testing different combinations of best-pixel image composites and spectral metrics, based on all available observations, highlighted the strength of using multiple seasons in combination with spectral metrics for land-cover classifications. The Landsat 8 data record is thus very promising for up-to-date, large-area, yet fine-grained connectivity assessments. This highlights the value of the Landsat archives for large mammal conservation, and conservation planning, and suggests that these archives are currently an underused resource in conservation science and application (Turner et al., 2015). For the Caucasus, our results suggest that protected areas are structurally connected through forests, but widespread bottlenecks and low corridor quality stress the need for immediate conservation planning and action to both, protect existing corridors and restore their quality. We identified corridors for three large mammal groups based on all Caucasian large mammals of high conservation priority, and this can be a useful starting point for such ground-based assessments (Beier et al., 2011), for example in the upcoming revision of the Caucasus Ecoregional Conservation Plan (Williams et al., 2006).

Habitat fragmentation is one of the main causes of global biodiversity loss. Therefore, monitoring habitat connectivity consistently over large areas can provide an important mechanism to track threat to biodiversity and potentially biodiversity change, and contribute to the standardized monitoring proposed under the essential biodiversity variable framework (Skidmore et al., 2015). Our approach demonstrates how Landsat 8 composites can contribute to such a global biodiversity monitoring strategy (Pettorelli et al., 2016).

Acknowledgements

B. Bleyhl gratefully acknowledges funding through an Elsa-Neumann scholarship from the Federal State of Berlin, Germany. V. Radeloff acknowledged support from the NASA Land Cover and Land Use Change Program. We thank H. Abolghasemi, D. Ashayeri, E. Askerov, E. Babaev, G. Bragina, A. Gavashelishvili, A. Ghoddousi, I. Khorozyan, B. Kiabi, C. Montalvo, U. Semenov, M. Soofi, P. Weinberg, and Y. Yarovenko for

participating in our expert consolidation email survey. We thank E. Askerov for helpful discussions and comments on an earlier version of the manuscript. We are also grateful to WWF Armenia, WWF Azerbaijan, WWF Caucasus Programme Office Georgia, and WWF Germany for logistic support during field trips. We are grateful for the help and constructive comments of two reviewers.

Appendix A. Supplementary data

Supplementary data to this article can be found online at http://dx.doi.org/10.1016/j.rse.2017.03.001.

References

Baumann, M., Gasparri, I., Piquer-Rodríguez, M., Gavier Pizarro, G., Griffiths, P., Hostert, P., Kuemmerle, T., 2016. Carbon emissions from agricultural expansion and intensification in the Chaco. Glob. Chang. Biol.

Baumann, M., Kuemmerle, T., Elbakidze, M., Ozdogan, M., Radeloff, V.C., Keuler, N.S., Prishchepov, A.V., Kruhlov, I., Hostert, P., 2011. Patterns and drivers of post-socialist farmland abandonment in Western Ukraine. Land Use Policy 28, 552–562.

Baumann, M., Ozdogan, M., Kuemmerle, T., Wendland, K.J., Esipova, E., Radeloff, V.C., 2012. Using the Landsat record to detect forest-cover changes during and after the collapse of the Soviet Union in the temperate zone of European Russia. Remote Sens. Environ. 124, 174–184.

Beier, P., Majka, D.R., Newell, S.L., 2009. Uncertainty analysis of least-cost modeling for designing wildlife linkages. Ecol. Appl. 19, 2067–2077.

Beier, P., Majka, D.R., Spencer, W.D., 2008. Forks in the road: choices in procedures for designing wildland linkages. Conserv. Biol. 22, 836–851.

Beier, P., Spencer, W., Baldwin, R.F., McRae, B.H., 2011. Toward best practices for developing regional connectivity maps. Conserv. Biol. 25, 879–892.

Bleyhl, B., Sipko, T., Trepet, S., Bragina, E., Leitao, P.J., Radeloff, V.C., Kuemmerle, T., 2015. Mapping seasonal European bison habitat in the Caucasus Mountains to identify potential reintroduction sites. Biol. Conserv. 191, 83–92.

Bragina, E.V., Ives, A.R., Pidgeon, A.M., Kuemmerle, T., Baskin, L.M., Gubar, Y.P., Piquer-Rodríguez, M., Keuler, N.S., Petrosyan, V.G., Radeloff, V.C., 2015. Rapid declines of large mammal populations after the collapse of the Soviet Union. Conserv. Biol. 184, 456–464.

Breiman, L., 2001. Random forests. Mach. Learn. 45, 5–32.

Brudvig, L.A., Damschen, E.I., Tewksbury, J.J., Haddad, N.M., Levey, D.J., 2009. Landscape connectivity promotes plant biodiversity spillover into non-target habitats. Proc. Natl. Acad. Sci. U. S. A. 106, 9328–9332.

Bruner, A.G., Gullison, R.E., Rice, R.E., da Fonseca, G.A.B., 2001. Effectiveness of parks in protecting tropical biodiversity. Science 291, 125–128.

Butchart, S.H.M., Walpole, M., Collen, B., Strien, A.v., Scharlemann, J.P.W., Almond, R.E.A., Baillie, J.E.M., Bomhard, B., Brown, C., Bruno, J., Carpenter, K.E., Carr, G.M., Chanson, J., Chenery, A.M., Csirke, J., Davidson, N.C., Dentener, F., Foster, M., Galli, A., Galloway, J.N., Genovesi, P., Gregory, R.D., Hockings, M., Kapos, V., Lamarque, J.-F., Leverington, F., Loh, J., McGeoch, M.A., McRae, L., Minasyan, A., Morcillo, M.H., Oldfield, T.E.E., Pauly, D., Quader, S., Revenga, C., Sauer, J.R., Skolnik, B., Spear, D., Stanwell-Smith, D., Stuart, S.N., Symes, A., Tierney, M., Tyrrell, T.D., Vié, J.-C., Watson, R., 2010. Global biodiversity: indicators of recent declines. Science 328, 1164–1168.

Crooks, K.R., Sanjayan, M. (Eds.), 2006. Connectivity Conservation. Cambridge University Press, Cambridge, UK.

De Leeuw, J., Jia, H., Yang, L., Liu, X., Schmidt, K., Skidmore, A.K., 2006. Comparing accuracy assessments to infer superiority of image classification methods. Int. J. Remote Sens. 27, 223–232.

DeFries, R., Hansen, A., Turner, B.L., Reid, R., Liu, J., 2007. Land use change around protected areas: management to balance human needs and ecological function. Ecol. Appl. 17, 1031–1038.

Di Marco, M., Boitani, L., Mallon, D., Hoffmann, M., Iacucci, A., Meijaard, E., Visconti, P., Schipper, J., Rondinini, C., 2014. A retrospective evaluation of the global decline of carnivores and ungulates. Conserv. Biol. 28, 1109–1118.

Di Minin, E., Hunter, L.T.B., Balme, G.A., Smith, R.J., Goodman, P.S., Slotow, R., 2013. Creating larger and better connected protected areas enhances the persistence of big game species in the Maputaland-Pondoland-Albany biodiversity hotspot. PLoS One 8, e71788.

Dickson, B.G., Roemer, G.W., McRae, B.H., Rundall, J.M., 2013. Models of regional habitat quality and connectivity for Pumas (*Puma concolor*) in the Southwestern United States. PLoS One 8.

Dutta, T., Sharma, S., McRae, B.H., Roy, P.S., DeFries, R., 2015. Connecting the dots: mapping habitat connectivity for tigers in central India. Reg. Environ. Chang. 1–15.

Estel, S., Kuemmerle, T., Alcantara, C., Levers, C., Prishchepov, A.V., Hostert, P., 2015. Mapping farmland abandonment and recultivation across Europe using MODIS NDVI time series. Remote Sens. Environ.

Foody, G.M., 2002. Status of land cover classification accuracy assessment. Remote Sens. Environ. 80, 185–201.

Gilbert-Norton, L., Wilson, R., Stevens, J.R., Beard, K.H., 2010. A meta-analytic review of corridor effectiveness. Conserv. Biol. 24, 660–668.

Giovarelli, R., Bledsoe, D., 2001. Land Reform in Eastern Europe. Report. Rural Development Institute (RDI), Seattle.

Gislason, P.O., Benediktsson, J.A., Sveinsson, J.R., 2006. Random forests for land cover classification. Pattern Recogn. Lett. 27, 294–300.

Griffiths, P., Kuemmerle, T., Baumann, M., Radeloff, V.C., Abrudan, I.V., Lieskovsky, J., Munteanu, C., Ostapowicz, K., Hostert, P., 2014. Forest disturbances, forest recovery, and changes in forest types across the Carpathian ecoregion from 1985 to 2010 based on Landsat image composites. Remote Sens. Environ. 151, 72–88.

Griffiths, P., Mueller, D., Kuemmerle, T., Hostert, P., 2013a. Agricultural land change in the Carpathian ecoregion after the breakdown of socialism and expansion of the European Union. Environ. Res. Lett. 8, 045024.

Griffiths, P., van der Linden, S., Kuemmerle, T., Hostert, P., 2013b. A pixel-based Landsat compositing algorithm for large area land cover mapping. IEEE J. Sel. Top. Appl. Earth Observ. Remote. Sens. 6, 2088–2101.

Haddad, N.M., Bowne, D.R., Cunningham, A., Danielson, B.J., Levey, D.J., Sargent, S., Spira, T., 2003. Corridor use by diverse taxa. Ecology 84, 609–615.

Hansen, M.C., Potapov, P.V., Moore, R., Hancher, M., Turubanova, S.A., Tyukavina, A., Thau, D., Stehman, S.V., Goetz, S.J., Loveland, T.R., Kommareddy, A., Egorov, A., Chini, L., Justice, C.O., Townshend, J.R.G., 2013. High-resolution global maps of 21st-century forest cover change. Science 342, 850–853.

Hermosilla, T., Wulder, M.A., White, J.C., Coops, N.C., Hobart, G.W., 2015. Regional detection, characterization, and attribution of annual forest change from 1984 to 2012 using Landsat-derived time-series metrics. Remote Sens. Environ. 170, 121–132.

Hilty, J.A., Lidicker Jr., W.Z., Merenlender, A.M., 2006. Corridor Ecology: The Science and Practice of Linking Landscapes for Biodiversity Conservation. Island Press, Washington, DC.

IUCN, & UNEP-WCMC, 2015. The World Database on Protected Areas (WDPA). WCMC, Cambridge, UK.

Jones, D.A., Hansen, A.J., Bly, K., Doherty, K., Verschuyl, J.P., Paugh, J.I., Carle, R., Story, S.J., 2009. Monitoring land use and cover around parks: a conceptual approach. Remote Sens. Environ. 113, 1346–1356.

Khorozyan, I.G., Abrarnov, A.V., 2007. The Leopard, *Panthera pardus*, (Carnivora: Felidae) and its resilience to human pressure in the Caucasus. Zool. Middle East 41, 11–24.

Koen, E.L., Garroway, C.J., Wilson, P.J., Bowman, J., 2010. The effect of map boundary on estimates of landscape resistance to animal movement. PLoS One 5, e11785.

Krever, V., Zazanashvili, N., Jungius, H., Williams, L., Petelin, D. (Eds.), 2001. Biodiversity of the Caucasus Ecoregion: An Analysis of Biodiversity and Current Threats and Initial Investment Portfolio. World Wide Fund for Nature, Baku, Erevan, Gland, Moscow, Tbilisi.

Lerman, Z., Csaki, C., Feder, G., 2004. Agriculture in Transition: Land Policies and Evolving Farm Structures in Post-Soviet-countries. Lexington Books, Landham, MD.

Macdonald, D.W., Johnson, P.J., Albrechtsen, L., Seymour, S., Dupain, J., Hall, A., Fa, J.E., 2012. Bushmeat trade in the Cross-Sanaga rivers region: evidence for the importance of protected areas. Biol. Conserv. 147, 107–114.

McRae, B.H., 2012. Pinchpoint Mapper Connectivity Analysis Software. The Nature Conservancy, Seattle, WA.

McRae, B.H., Dickson, B.G., Keitt, T.H., Shah, V.B., 2008. Using circuit theory to model connectivity in ecology, evolution, and conservation. Ecology 89, 2712–2724.

McRae, B.H., Kavanagh, D.M., 2011. Linkage Mapper User Guide. The Nature Conservancy, Seattle, WA.

McRae, B.H., Shah, V.B., Mohapatra, 2013. Circuitscape 4 User Guide. The Nature Conservancy.

Montalvo Mancheno, C.S., Zazanashvili, N., Beruchashvili, G., 2016. Effectiveness of the network of protected areas of the South Caucasus at representing terrestrial ecosystems after the dissolution of the Soviet Union. Environ. Conserv. 1–8.

Müller, H., Rufin, P., Griffiths, P., Barros Siqueira, A.J., Hostert, P., 2015. Mining dense Landsat time series for separating cropland and pasture in a heterogeneous Brazilian savanna landscape. Remote Sens. Environ. 156, 490–499.

Olofsson, P., Foody, G.M., Herold, M., Stehman, S.V., Woodcock, C.E., Wulder, M.A., 2014. Good practices for estimating area and assessing accuracy of land change. Remote Sens. Environ. 148, 42–57.

Pelletier, D., Clark, M., Anderson, M.G., Rayfield, B., Wulder, M.A., Cardille, J.A., 2014. Applying circuit theory for corridor expansion and management at regional scales: tiling, pinch points, and omnidirectional connectivity. PLoS One 9, 11.

Pettorelli, N., Laurance, W.F., O'Brien, T.G., Wegmann, M., Nagendra, H., Turner, W., 2014. Satellite remote sensing for applied ecologists: opportunities and challenges. J. Appl. Ecol. 51, 839–848.

Pettorelli, N., Wegmann, M., Skidmore, A., Mücher, S., Dawson, T.P., Fernandez, M., Lucas, R., Schaepman, M.E., Wang, T., O'Connor, B., Jongman, R.H.G., Kempeneers, P., Sonnenschein, R., Leidner, A.K., Böhm, M., He, K.S., Nagendra, H., Dubois, G., Fatoyinbo, T., Hansen, M.C., Paganini, M., de Klerk, H.M., Asner, G.P., Kerr, J.T., Estes, A.B., Schmeller, D.S., Heiden, U., Rocchini, D., Pereira, H.M., Turak, E., Fernandez, N., Lausch, A., Cho, M.A., Alcaraz-Segura, D., McGeoch, M.A., Turner, W., Mueller, A., St-Louis, V., Penner, J., Vihervaara, P., Belward, A., Reyers, B., Geller, G.N., 2016. Framing the concept of satellite remote sensing essential biodiversity variables: challenges and future directions. Remote. Sens. Ecol. Conserv.

Potapov, P., Turubanova, S., Hansen, M.C., 2011. Regional-scale boreal forest cover and change mapping using Landsat data composites for European Russia. Remote Sens. Environ. 115, 548–561.

Potapov, P.V., Turubanova, S.A., Tyukavina, A., Krylov, A.M., McCarty, J.L., Radeloff, V.C., Hansen, M.C., 2015. Eastern Europe's forest cover dynamics from 1985 to 2012 quantified from the full Landsat archive. Remote Sens. Environ. 159, 28–43.

Prishchepov, A.V., Radeloff, V.C., Dubinin, M., Alcantara, C., 2012. The effect of Landsat ETM/ETM plus image acquisition dates on the detection of agricultural land abandonment in Eastern Europe. Remote Sens. Environ. 126, 195–209.

Ripple, W.J., Estes, J.A., Beschta, R.L., Wilmers, C.C., Ritchie, E.G., Hebblewhite, M., Berger, J., Elmhagen, B., Letnic, M., Nelson, M.P., Schmitz, O.J., Smith, D.W., Wallach, A.D.,

Wirsing, A.J., 2014. Status and ecological effects of the world's largest carnivores. Science 343, 1241484.
Ripple, W.J., Newsome, T.M., Wolf, C., Dirzo, R., Everatt, K.T., Galetti, M., Hayward, M.W., Kerley, G.I.H., Levi, T., Lindsey, P.A., Macdonald, D.W., Malhi, Y., Painter, L.E., Sandom, C.J., Terborgh, J., Van Valkenburgh, B., 2015. Collapse of the world's largest herbivores. Sci. Adv. 1, e1400103.
Roy, D.P., Ju, J.C., Kline, K., Scaramuzza, P.L., Kovalskyy, V., Hansen, M., Loveland, T.R., Vermote, E., Zhang, C.S., 2010. Web-enabled Landsat Data (WELD): Landsat ETM plus composited mosaics of the conterminous United States. Remote Sens. Environ. 114, 35–49.
Sanderson, J., da Fonseca, G.a.B., Galindo-Leal, C., Alger, K., Inchausty, V.H., Morrison, K., Rylands, A., 2006. Escaping the minimalist trap: design and implementation of large-scale biodiversity corridors. In: Crooks, K.R., Sanjayan, M. (Eds.), Connectivity Conservation. Cambridge University Press, Cambridge, UK.
Senf, C., Leitao, P.J., Pflugmacher, D., van der Linden, S., Hostert, P., 2015. Mapping land cover in complex Mediterranean landscapes using Landsat: improved classification accuracies from integrating multi-seasonal and synthetic imagery. Remote Sens. Environ. 156, 527–536.
Skidmore, A.K., Pettorelli, N., Coops, N.C., Geller, G.N., Hansen, M., Lucas, R., Mucher, C.A., O'Connor, B., Paganini, M., Pereira, H.M., Schaepman, M.E., Turner, W., Wang, T.J., Wegmann, M., 2015. Agree on biodiversity metrics to track from space. Nature 523, 403–405.
Turner, W., Rondinini, C., Pettorelli, N., Mora, B., Leidner, A.K., Szantoi, Z., Buchanan, G., Dech, S., Dwyer, J., Herold, M., Koh, L.P., Leimgruber, P., Taubenboeck, H., Wegmann, M., Wikelski, M., Woodcock, C., 2015. Free and open-access satellite data are key to biodiversity conservation. Biol. Conserv. 182, 173–176.
Walker, R., Craighead, L., 1997. Analyzing wildlife movement corridors in Montana using GIS. Proceedings of the 1997 ESRI European User Conference, pp. 1–18 (Copenhagen).
Watson, J.E.M., Dudley, N., Segan, D.B., Hockings, M., 2014. The performance and potential of protected areas. Nature 515, 67–73.
White, J.C., Wulder, M.A., Hobart, G.W., Luther, J.E., Hermosilla, T., Griffiths, P., Coops, N.C., Hall, R.J., Hostert, P., Dyk, A., Guindon, L., 2014. Pixel-based image compositing for large-area dense time series applications and science. Can. J. Remote. Sens. 40, 192–212.
Wiens, J., Sutter, R., Anderson, M., Blanchard, J., Barnett, A., Aguilar-Amuchastegui, N., Avery, C., Laine, S., 2009. Selecting and conserving lands for biodiversity: the role of remote sensing. Remote Sens. Environ. 113, 1370–1381.
Williams, L., Zazanashvili, N., Sanadiradze, G., Kandaurov, A. (Eds.), 2006. Ecoregional Conservation Plan for the Caucasus. WWF, KfW, BMZ, CEPF, MacArthur Foundation, Tbilisi.
Wulder, M.A., Coops, N.C., 2014. Make earth observations open access. Nature 513, 30–31.
Wulder, M.A., White, J.C., Loveland, T.R., Woodcock, C.E., Belward, A.S., Cohen, W.B., Fosnight, E.A., Shaw, J., Masek, J.G., Roy, D.P., 2015. The global Landsat archive: status, consolidation, and direction. Remote Sens. Environ. 185, 271–283.
Zazanashvili, N., Garforth, M., Jungius, H., Gamkrelidze, T. (Eds.), 2012. Ecoregion Conservation Plan for the Caucasus, 2012 revised updated ed. WWF, KfW, BMZ, Tbilisi.
Zazanashvili, N., Nakhutsrishvili, G., Gagnidze, R., 2000. Main types of vegetation zonation on the mountains of the Caucasus. Acta Phytogeographica Suecica 85, 7–16.
Zazanashvili, N., Sanadiradze, G., Bukhnikashvili, A., Kandaurov, A., Tarkhnishvili, D., 2004. Caucasus. In: Mittermeier, R.A., Gil, P.R., Hoffmann, M., Pilgrim, J., Brooks, T., Mittermeier, C.G., Lamoreux, J., da Fonseca, G.a.B. (Eds.), Hotspots Revisited: Earth's biologically Richest and Most Endangered Terrestrial Ecoregions. CEMEX/Agrupacion Sierra Madre, Mexico City, Mexico.
Zeller, K.A., McGarigal, K., Whiteley, A.R., 2012. Estimating landscape resistance to movement: a review. Landsc. Ecol. 27, 777–797.
Ziółkowska, E., Ostapowicz, K., Radeloff, V.C., Kuemmerle, T., 2014. Effects of different matrix representations and connectivity measures on habitat network assessments. Landsc. Ecol. 29, 1551–1570.
Ziółkowska, E., Ostapowicz, K., Radeloff, V.C., Kuemmerle, T., Sergiel, A., Zwijacz-Kozica, T., Zięba, F., Śmietana, W., Selva, N., 2016a. Assessing differences in connectivity based on habitat versus movement models for brown bears in the Carpathians. Landsc. Ecol. 1–20.
Ziółkowska, E., Perzanowski, K., Bleyhl, B., Ostapowicz, K., Kuemmerle, T., 2016b. Understanding unexpected reintroduction outcomes: Why aren't European bison colonizing suitable habitat in the Carpathians? Biol. Conserv. 195, 106–117.